Electrochemical Sensing of Membrane Potential and Enzyme Function Using Gallium Arsenide Electrodes Functionalized with Supported Membranes

Daniel Gassull,[†,‡] Abraham Ulman,[§] Michael Grunze,[||] and Motomu Tanaka*[,†,‡]

Biophysical Chemistry II, Institute of Physical Chemistry and BIOQUANT, University of Heidelberg, D69120 Heidelberg, Germany, Department of Physics, Technical University Munich, D85748 Garching, Germany, Department of Chemical and Biological Sciences, Polytechnic University, Six Metrotech Center, Brooklyn, New York 11201, Applied Physical Chemistry, Institute of Physical Chemistry, University of Heidelberg, D69120 Heidelberg, Germany

Received: November 20, 2007; In Final Form: January 25, 2008

We deposit phospholipid monolayers on highly doped p-GaAs electrodes that are precoated with methyl-mercaptobiphenyl monolayers and operate such a biofunctional electrolyte-insulator-semiconductor (EIS) setup as an analogue of a metal-oxide-semiconductor setup. Electrochemical impedance spectra measured over a wide frequency range demonstrate that the presence of a lipid monolayer remarkably slows down the diffusion of ions so that the membrane-functionalized GaAs can be subjected to electrochemical investigations for more than 3 days with no sign of degradation. The biofunctional EIS setup enables us to translate changes in the surface charge density Q and bias potentials U_{bias} into the change in the interface capacitance C_p. Since C_p is governed by the capacitance of semiconductor space charge region C_{SC}, the linear relationships obtained for 1/Cp2 vs Q and $1/C_p^2$ vs U_{bias} suggests that C_p can be used to detect the surface charges with a high sensitivity (1 charge per 18 nm^2). Furthermore, the kinetics of phospholipids degradation by phospholipase A_2 can also be monitored by a significant decrease in diffusion coefficients through the membrane by a factor of 104. Thus, the operation of GaAs membrane composites established here allows for electrochemical sensing of surface potential and barrier capability of biological membranes in a quantitative manner.

Introduction

Functional modification of solid-based devices with biomolecules draws an increasing attention toward creation of hybrid sensor materials, which enable one to translate specific functions of biomolecules into electrical current readouts.[1,2] Semiconductors offer unique advantages over metals, because in semiconductors changes in the surface potential caused by biochemical reactions can be sensitively detected by changes in the electric structures. Moreover, the recent development of semiconductor technology allows for flexible band gap engineering of highly sensitive, low-dimensional devices (such as nanowires, two-dimensional electron gases). Gallium arsenide (GaAs) is one of the most commonly used device materials for high electron mobility transistors (HEMTs) because: (i) GaAs undergoes almost no lattice strain in fabrication of alloys (e.g., $Al_xGa_{1-x}As$), and (ii) GaAs-based devices can be operated at high frequency at a very low thermal noise in comparison to Si-based devices.[3−5] Applications of GaAs-based devices in liquid-phase sensors under biologically relevant conditions, however, have been impeded by its intrinsic instability in aqueous electrolytes near neutral pH.[6−8]

We overcame this problem by deposition of organic thiol monolayers.[9−12] We previously reported that the same functionalization protocols can be adopted not only on bulk GaAs electrodes but also on InAs quantum dots 10 nm below the GaAs surface as well as on two-dimensional electron gas (2DEG) under 60 nm thick GaAs cap layer.[13] 2DEG devices coated with 1 nm thick biphenylthiol monolayers can be operated in aqueous buffer for more than 10 h with no sign of degradation, in contrast to naked devices that show continuous and irreversible degradation within 1 h. In our recent account,[14] we further demonstrated that bulk GaAs electrodes coated with hydrophobic biphenylthiol monolayers can sensitively detect the electrolyte pH, which can be attributed to the adsorption of OH^- ions on surfaces coated with highly ordered monolayer of hydrophobic molecules. Notably, the pH sensitivity of bulk GaAs (35 mV/pH) is comparable to that of 2DEG devices.

In this study, we deposit phospholipid monolayers on GaAs electrodes, which are precoated with hydrophobic 4′-methyl-4-biphenylthiol (CH_3−MBP) monolayers (Scheme 1). Because of a highly insulating property of CH_3−MBP monolayers (the resistance of the interface after monolayer deposition is as high as 2−3 MΩ cm^2) as well as phospholipid membranes (the resistance of a defect-free membrane is typically ∼ 1 MΩ cm^2), the whole interface can be treated as an analogue of electrolyte-insulator-semiconductor (EIS) structures, so that changes in the surface potentials can be detected as changes in semiconductor space charge capacitance. On the other hand, the enzymatic degradation of a lipid monolayer by phospholipase A_2 (PLA_2) can be monitored by changes in the membrane permeability (diffusion coefficient of ions across the membrane). The details of the obtained results are described in the following sections.

Materials and Methods

Materials. Single-crystalline Zn-doped (p-doped) GaAs [100] wafers with a doping ratio of 2.2−3.5 × 10^{19} cm^{-3} were

* To whom correspondence should be addressed. E-mail: tanaka@uni-heidelberg.de. Fax: +49 6221544918.
† Institute of Physical Chemistry and BIOQUANT, University of Heidelberg.
‡ Technical University Munich.
§ Polytechnic University.
|| Institute of Physical Chemistry, University of Heidelberg.

10.1021/jp711068b CCC: $40.75
Published on Web 04/16/2008

SCHEME 1: Schematic Illustrations of the Two Experimental Systems[a]

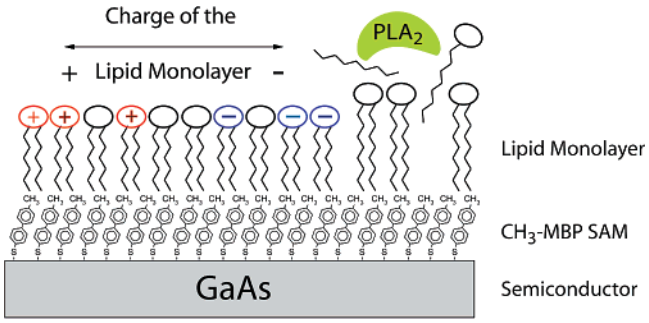

[a] Over a SAM of CH_3-MBP, a phospholipid monolayer is spread by vesicle fusion. In the first system (left), changes in the surface charge density (i.e., surface potential) are detected as changes in the space charge capacitance of semiconductors. On the other hand, the enzymatic degradation of a lipid monolayer by PLA_2 can be monitored by changes in the membrane permeability (diffusion coefficient of ions across the membrane).

purchased from Wafer Technology Ltd. (Bucks, U.K.). For these electrochemical studies, an Ohmic contact was established from the back side of the wafer by electron beam vapor deposition of Ni (100 Å), Ge (200 Å), and Au (2500 Å). The synthesis of methyl-mercaptobiphenyl (CH_3-MBP) is reported elsewhere.[15] 1,2-Dimyristoyl-*sn*-glycero-3-phosphocholine (DMPC), dihexadecyl-dimethylammoniumbromide (DHDAB), 1,2-dimyristoyl-*sn*-glycero-3-[phospho-rac-(1-glycerol)] (DMPG), and cholesterol were purchased from Avanti Polar Lipids (Alabaster, Al, USA). All other chemicals were purchased from Sigma Aldrich (Steinheim, Germany) and were used without further modification. Freshly distilled Millipore water (18 MΩ cm) was used throughout this study.

Sample Preparation. Prior to the surface modification, the samples were briefly sonicated in acetone (~3 min) and rinsed with ethanol. The native oxide of GaAs was stripped by soaking the sample in concentrated HCl for 1 min, resulting in a stoichiometric GaAs surface.[16] Self-assembled monolayers were deposited by immersing freshly etched substrates into ethanol at 50 °C for 20 h. The reaction was carried out under nitrogen (N_2) atmosphere to avoid surface oxidation. After deposition, the sample was taken out from the reactor, sonicated briefly (~1 min) in ethanol, and dried by N_2 flow.

Lipids were dissolved in chloroform and mixed to the desired composition. To avoid the phase separation of lipids as well as to achieve high electric resistance, the molar fraction of cholesterol was always kept at 40%. After evaporation of chloroform, the sample was kept overnight in vacuum and was suspended in the buffer to achieve a concentration of 1 mg/mL. Small unilamellar vesicles were prepared by sonication of lipid suspensions for 15−25 min, and the resulting vesicle suspension was injected in the flow chamber.

Electrochemical Impedance Spectroscopy. The electrochemical properties of the surfaces of chemically functionalized GaAs electrodes before and after the deposition of lipid monolayers were monitored by AC impedance spectroscopy at room temperature (Voltalab 40, Radiometer-Analytical, Lyon, France). The contact area of the surface with the electrolyte was 0.28 cm^2, and the volume inside the chamber was about 1.5 mL. An Ag/AgCl electrode was used as a reference electrode and an Au electrode as a counter electrode. For each electrochemical measurement, the current minimum potential determined by cyclic voltammetry $U_{bias,j=0} = -400$ mV was applied vs a Ag/AgCl reference electrode in order to minimize the irreversible electrochemical degradation of GaAs electrodes.[9] Instead of using a rotating disk electrode, a constant flow of degassed 10 mM phosphate buffer with 150 mM of NaCl was applied. Impedance spectra were measured between 100 kHz and 100 mHz, under a sinusoidal potentials with an amplitude of 10 mV. To estimate the electrochemical parameters quantitatively from the measured impedance data, we have used different simplified equivalent circuit elements models (Scheme 1). The ratio between the absolute error and absolute value (in percentage) for each parameter after fitting an impedance spectrum is within ±1%, and the cumulative error taking all parameters into account (called "fitting error" in the following) is kept within ±5% throughout the study.

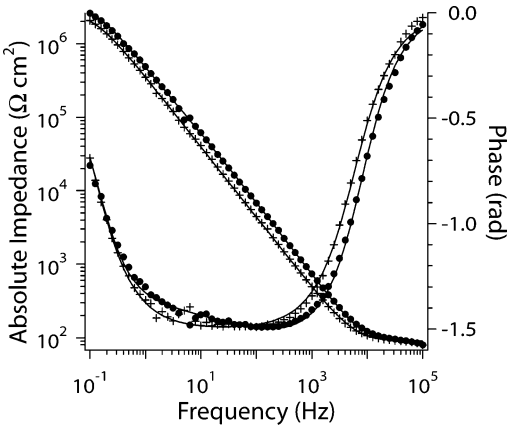

Figure 1. Impedance spectra (Bode plot) before (+) and after (●) the deposition of a lipid monolayer on a GaAs electrode coated with a CH_3-MBP monolayer, recorded at the current minimum potential ($U_{bias,j=0} = -400$ mV). The solid lines correspond to the fitting results using model A (+) and model B (●) in Scheme 2.

Results and Discussion

Prior to the lipid membrane deposition, we check the electrochemical stability of each GaAs sample coated with a methyl-mercaptobiphenyl (CH_3-MBP) monolayer with impedance spectroscopy.[11] To quantitatively identify various electrochemical layers, measurements are carried out in a wide frequency range (10^5-10^{-1} Hz) at the current minimum potential $U_{bias,j=0} = -400$ mV (vs Ag/AgCl), determined by cyclic voltammetry.[9,11] Instead of *n*-GaAs used in our previous studies, we use *p*-GaAs as an electrode in this study. Thus, the current minimum potential of the *p*-GaAs sample, i.e., the bias potential at which the sum of the oxidative and reductive currents is minimum, is determined by cyclic voltammetry to be $U_{bias,j=0} = -400$ mV (vs Ag/AgCl).

Only the samples that show negligibly small deviations (within ±1%) in interface resistance and capacitance over several scans are subjected to the further functionalization steps.

Electrochemical Characterization of Lipid Monolayer on GaAs. Figure 1 represents the absolute impedance and the phase shift plotted as a function of frequency (Bode plot) of the GaAs coated with CH_3-MBP before (+) and after (●) the deposition of a lipid monolayer. To analyze the measured impedance spectra, we take two different circuit models that are presented in Scheme 2. As we described in our previous accounts more in detail[10,11,14] the impedance spectra before the membrane deposition (+) can be well fitted by taking Model A (solid lines). R_s reflects the Ohmic resistance of the electrolyte and/or electronic contacts in the high-frequency regime ($f > 10^5$ Hz), while C_p and R_p characterize the capacitance and resistance of the solid/electrolyte interface, respectively. The fitting yields

SCHEME 2: Equivalent Circuit Models Used to Fit the Impedance Spectra[a]

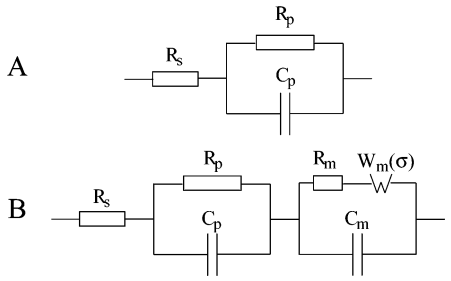

[a] Model A consists of resistance of electrolyte and ohmic contact R_s, interface capacitance C_p, and interface resistance R_p. For analyzing impedance spectra in the presence of a lipid monolayer, we use model B that additionally includes Warburg element $W_m(\sigma)$, the phase transition resistance at the electrolyte/membrane interface R_{pt}, and the membrane capacitance C_m.

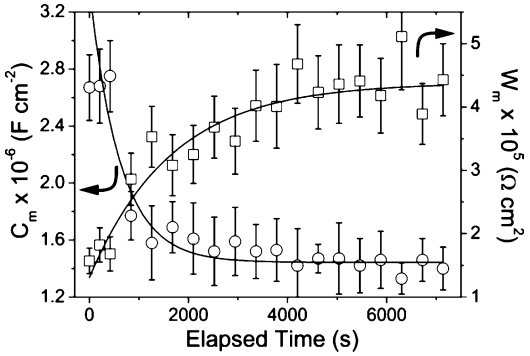

Figure 2. Kinetics of the formation of a phospholipid monolayer on a GaAs electrode coated with a CH_3−MBP monolayer. At $t = 0$, vesicle suspension was injected to the electrochemical cell, and changes in the Warburg element W_m (□) and the membrane capacitance C_m (○) are recorded as a function of time. Both W_m and C_m reached to the saturation level at $t \approx 7000$ s. Such time evolutions can be fitted empirically with a first-order exponential function, yielding the characteristic time constants of $\tau_{W_m} = 1350 \pm 200$ s for W_m and $\tau_{C_m} = 310 \pm 30$ s for C_m, respectively.

the interface capacitance and resistance of interface to be $R_p = 1.2$ MΩ cm^2 and $C_p = 1.9$ μFcm^{-2}, respectively.

Here, the interface capacitance, C_p, can be simplified to a serial connection of capacitance of the electrolyte (Gouy−Chapman−Stern capacitance), C_{GCS}, capacitance of the self-assembled monolayer (SAM), C_{SAM}, and space charge capacitance of the semiconductor, C_{SC}. Here, C_{GCS} is a serial connection of the Helmholtz layer capacitance, $C_H \geq 140$ μFcm^{-2}, and the diffusion layer capacitance, $C_{diff} \geq 0.9$ Fcm^{-2}. Moreover, our preliminary simulation with the detailed model[7,10] implied that the capacitive contribution from the surface states, C_{SS}, is negligible in our experimental system. Thus, we conclude that C_p of the freshly etched, bare GaAs (which has the doping ratio of $n_A{}^p \approx 3 \times 10^{19}$ cm^{-3}) is governed by C_{SC}, which is in the range of 1.5−2.5 μF cm^{-2}.

As presented in Figure 2 in more detail, the impedance spectra of the sample with a lipid monolayer (containing 60 mol % DMPC and 40 mol % cholesterol) reach the saturation level (●) about 2 h after the injection of vesicle suspensions. As we reported in our previous account,[17] the best fit can be achieved by taking model B (Scheme 2), which includes a new set of circuit elements representing the phase transition resistance at the electrolyte/membrane interface (R_{PT}), membrane capacitance (C_m), and so-called Warburg resistance (W_m). The Warburg resistance, W_m, is introduced in order to account for the diffusion of ions across the membrane.[18,19] In fact, the fit without Warburg resistance, i.e., with a parallel pair of Ohmic resistance and capacitance, results in a large fitting error (±15%).

Analytically, the Warburg resistance can be expressed as[20]

$$W_m(\omega) = \sigma(1 - i)\omega^{-1/2} \quad (1)$$

where σ is the Warburg parameter

$$\sigma = \frac{4RT}{\sqrt{2}F^2n^2\rho A}\frac{1}{\sqrt{D}} \quad (2)$$

A is the active electrode area, D the diffusion constant of the ions across the interface, ρ their concentration at the surface, and ω the angular frequency of the read-out signal. The constants R, T, n, and F have their usual meanings.

Taking this model, the electrochemical parameters of a lipid monolayer can be calculated to be $R_{PT} = 9 \times 10^2$ Ω cm^2, $C_m = 1.5$ μF cm^{-2}, and $W_m = 4.2 \times 10^5$ Ω cm^2. Note that R_{PT} merely represents the resistance of the electrolyte/membrane interface, which does not include the diffusion barrier characteristics of the hydrophobic core region of the membrane. Here, the barrier capability of the membrane against the diffusion of ions can be represented by diffusion coefficients and thus W_m. If one assumes that the concentration of ions on the surface is comparable to that in the bulk electrolyte, a diffusion constant of $D_m = 5 \times 10^{-5}$ μm^2 s^{-1} can be calculated from the Warburg constant, $\sigma_m = (5 \pm 0.5) \times 10^5$ Ω s$^{1/2}$. This diffusion coefficient is about 7 orders of magnitude smaller than the diffusion of ions in aqueous electrolyte, $D = 1 \times 10^3$ μm^2 s^{-1} (calculated from the Stokes−Einstein equation of the ion with the radius of 3.5 Å) and about 3−4 orders of magnitude smaller than those across alkylsiloxiane monolayers, $D = 0.01-0.1$ μm^2 s^{-1}.[21] Such a significantly high Warburg resistance coincides with the excellent electrochemical stability achieved by the deposition of a lipid monolayer, where we observe no sign of electrochemical instability for more than 3 days within the experimental limit.

Recent X-ray[22] and neutron[23] reflectivity studies reported the presence of a thin gaseous layer at the interface between a hydrophobic surface and an aqueous electrolyte. However, the presence of such a layer cannot be detected by the impedance spectroscopy. It should be noted that the fitting of the impedance spectrum after the deposition of a lipid monolayer (Figure 1, ●) with model B, both R_p and C_p are kept floating. Here, the standard deviation between the C_p value obtained with model B (2.1 μF cm^{-2}) and the corresponding value calculated from the spectrum before the membrane deposition (Figure 1, +) with Model A (1.9 μF cm^{-2}) is within ±10%. In fact, we recently reported that the interface resistance of the GaAs electrode coated with a CH_3−MBP monolayer shows linear relationships with electrolyte pH and bias potential in a reproducible manner.[14] Such reproducible pH sensitivity cannot be achieved or accounted in the presence of a gaseous layer. Furthermore, the calculated capacitance of a lipid monolayer, $C_m = 1.5$ μF cm^{-2}, is almost double of the capacitance value reported for free-standing[24,25] and supported lipid bilayers,[26] $C_{bilayer} = 0.7$ μF cm^{-2}, which confirms the formation of a lipid monolayer on GaAs electrode coated with a CH_3−MBP monolayer. By assumption that the dielectric constant of the hydrocarbon chains is $\epsilon = 2.2$,[24,25,27] the thickness of the hydrocarbon region of a lipid membrane can be calculated to be $d_m = 12$ Å according to

$$C_m = \epsilon_m\epsilon_0/d_m \quad (3)$$

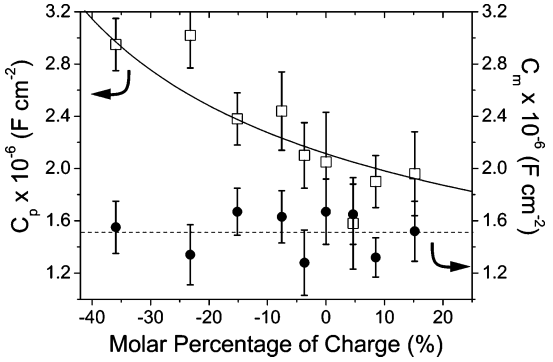

Figure 3. Dependence of membrane capacitance C_m (●) and interface capacitance C_p (□) on the doping ratios of charged lipids. Here, the signs in the x axis coincide with the signs of charges. It should be noted that C_m remains almost independent from the charge density on the membrane surface, $C_m = (1.5 \pm 0.2) \times \mu$F cm^{-2} (broken line). In contrast, C_p shows a clear dependence on the surface charge density, which seems to scale with [charged lipid]$^{-0.5}$ (solid line).

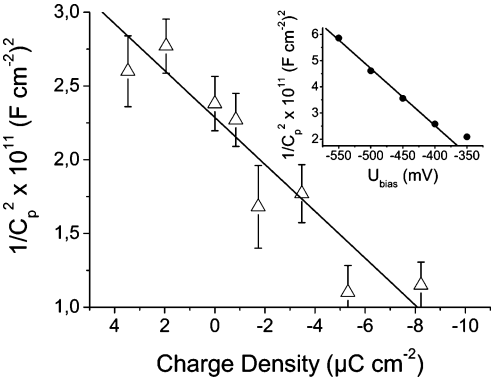

Figure 4. Plot of $1/C_p^2$ vs lateral charge density Q. Lateral charge density (note the sign of the x axis is inverted for the correspondence to "bias" potentials vs a reference electrode) can be calculated from the molar fraction of charged lipids using the known mean molecular area of a phospholipid (~70 Å^2).[31] For comparison, $1/C_p^2$ vs U_{bias} plot of a neutral lipid monolayer ($Q = 0\ \mu$C cm^{-2}) is presented as the inset, from which the carrier concentration $n_p = 1.1 \pm 0.3 \times 10^{19}$ cm^{-3} and the flat band potential $U_{FB} = -230 \pm 30$ mV can be calculated. This enables one to estimate the sensitivity of a membrane charge sensor to be 8 mV cm$^2/\mu$C, corresponding to 1 charge per 18 nm^2.

This seems to be in good agreement with the corresponding values reported previously.[17,28,29]

Kinetics of Membrane Formation. Figure 2 represents the plots of $W_m(\sigma)$ and C_m as a function of time, corresponding to the formation of a phospholipid monolayer. Each data point is calculated from individual impedance spectra collected every 7.5 min. About 7000 s after the injection of lipid vesicles (at $t = 0$), both W_m and C_p reach the saturation levels, i.e., the prolonged incubation time and the increase of the sample temperature do not lead to any change. Flushing of remaining vesicles from the flow chamber does not result in any change in both parameters, suggesting that vesicles adsorbed on the surface, even if they exist, do not influence the electrochemical characteristics of the supported membrane. By use of the surface plasmon resonance and quartz crystal microbalance, Keller et al. reported that the kinetics of supported membrane formation on a hydrophilic silica surface includes two steps: (i) adsorption of vesicles and (ii) spreading on the surface.[30] It should be noted that the kinetics observed here should mainly reflect the kinetics of the decrease of the active membrane area by spreading of the membrane on a hydrophobic surface, because the adhered vesicles cannot form the shielded "barrier" that significantly slows down the diffusion of ions. Empirical fitting of the observed kinetics with a first-order exponential function yields the characteristic time constants for W_m and C_p, $\tau_{W_m} = 1350 \pm 200$ s and $\tau_{C_m} = 310 \pm 30$ s, respectively. The apparent difference between the characteristic time constants obtained from changes in resistance and capacitance seems consistent with the qualitative tendency observed for the formation bilayer lipid membranes on Si/SiO_2 electrodes, where the capacitance reaches to its saturation level much faster than the resistance.[26]

Capacitive Sensing of Surface Charge Density. The effect of the charge density, Q, on C_p and C_m can be studied by changing the composition of lipids in a systematic manner. Here, the molar concentration of cholesterol is kept to be 40 mol %, and positively charged lipids (DHDAB) or negatively charged lipids (DMPG) are mixed with zwitterionic DMPC matrix to achieve the total lipid fraction to be 60 mol %. Figure 3 represents the C_p and C_m values plotted as a function of molar percentage of charged lipids. Note that the sign in the x-axis coincides with the sign of net surface charges, and the standard deviation of the electrochemical parameter after out of at least three independent experiments (experimental error) falls within ±10%.

As presented in the figure, the capacitance of a lipid monolayer (C_m) is almost independent from the mole fraction of charged lipids, $C_m = 1.5 \pm 0.2\ \mu$F cm^{-2} (the broken line in Figure 3). In contrast, C_p, which is dominated by the semiconductor space charge capacitance, shows a systematic dependence on the charge density on the membrane Q. As indicated by the solid line in Figure 3, the dependence of C_p on the lateral charge density and thus on the mole fraction of charged lipids seems to be well fitted with

$$C_p \propto \frac{1}{\sqrt{[\text{lipid}_{\text{charged}}]}} \tag{4}$$

It is also noteworthy that both Warburg resistance W_m and characteristic time constants for the membrane formation (τ_{W_m} and τ_{C_m}) remain constant irrespective of the presence of charged lipids, confirming that the electric resistance of the membrane (i.e., surface coverage) and kinetics of membrane formation are not influenced by the lipid compositions.

Since C_m can be quantitatively separated from C_p, this capacitance reflects the serial connection of the capacitance of a CH_3−MBP monolayer, C_{SAM}, and the semiconductor space charge capacitance, C_{SC}. In Figure 4, the influence of surface charge density on C_p is presented by plotting $1/C_p^2$ vs lateral charge density. Here, the mole fractions of charged lipids are converted to the charge density by taking the mean area occupied by one phospholipid molecule in the fluid phase (~70 Å^2 per molecule).[31,32] Therefore, this can be treated as an analogue of Mott−Shottky plots that predict a linear relationship between $1/C_p^2$ vs U_{bias}, if the semiconductor is operated at the depletion regime. In our experimental system, applications of various U_{ext} mean changes in the surface potential Ψ_S due to changes in the surface charge density Q according to the Poisson's equation.

To verify this hypothesis, we also measure the impedance spectra of a neutral lipid monolayer (consisting of 40 mol % cholesterol and 60 mol % DMPC) under various bias potentials. The impedance spectra are collected between $U_{bias} = -550$ and -350 mV, where the electrochemical stability of the system is guaranteed for more than a day. Here, U_{ext} is quantitatively represented by U_{bias}. As presented in the inset of Figure 4, the plot of $1/C_p^2$ vs U_{bias} shows a linear relationship. The slope of

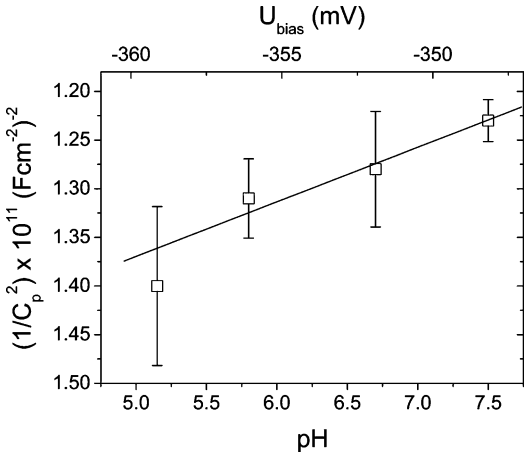

Figure 5. pH sensitivity of a GaAs electrode coated with a phospholipid monolayer. In contrast to a high pH sensitivity before the deposition of a lipid monolayer (GaAs with a CH_3-MBP monolayer has the sensitivity of 35 mV pH^{-1}),[14] the obtained pH sensitivity (4.7 mV pH^{-1}) is negligibly small. This finding indicates that no adsorption of OH^- ions take place on uncorrelated phosphocholine headgroups.

such a plot coincides with the density of the majority carrier in semiconductor n_p since

$$\frac{1}{C_{SC}^{\ 2}} \propto \frac{1}{n_p}\left[U_{ext} - U_{FB} - \frac{kT}{e}\right] \qquad (5)$$

U_{ext} is the external potential and U_{FB} the flat band potential.[33] The linear relationship observed here qualitatively indicates that C_p is sensitive to the change in the surface charge density Q. Taking eq 5, the carrier density of n_p(lipid monolayer) = $(1.1 \pm 0.3) \times 10^{19}$ cm^{-3} can be estimated from the slope. Although the model circuit used here include a couple of fitting parameters, this value seems reasonable in comparison to the values obtained from two reference experiments on GaAs coated with CH_3-MBP SAM: (i) the carrier density of GaAs with a CH_3-MBP monolayer calculated in the same manner, n_p(SAM−GaAs/imp) = $(3.2 \pm 0.3) \times 10^{19}$ cm^{-3}, and (ii) the carrier density measured by a Hall measurement in air, n_p(Hall) = $(3.7 \pm 0.2) \times 10^{19}$ cm^{-3}. From the intercept of the extrapolated linear part with the x-axis, the flat band potential of GaAs coated with a lipid monolayer can be calculated to be U_{FB}(lipid monolayer) = −230 mV. A slight shift from the value of GaAs with the CH_3-MBP SAM, U_{FB}(SAM−GaAs) = −280 mV can be attributed to a potential drop across the hydrocarbon chain region.

From two linear relationships obtained from our experiments, $1/C_p^2$ vs Q (Figure 4, main panel) and $1/C_p^2$ vs U_{bias} (Figure 4, insets), the sensitivity of the membrane charge sensor on GaAs can be calculated to be 8 mV $cm^2/\mu C$. Taking the area per lipid molecules (70 $Å^2$) into account, the charge sensitivity can also be given as 1 charge per 18 nm^2. In fact, the sensitivity achieved here is slightly better than the one of ITO coated with polymer-supported lipid monolayer, 1 charge per 8 nm^2.[17]

In our previous account,[14] we reported that the interface resistance of a GaAs electrode coated with a CH_3-MBP monolayer shows linear relationships with electrolyte pH and bias potential in a reproducible manner, which can analytically be extrapolated to be 35 mVpH^{-1}. By use of different equivalent circuit models, we interpreted the mechanism of the observed pH sensitivity as the adsorption of OH^- ions on the highly ordered CH_3 headgroups of the CH_3-MBP monolayer. However, as presented in Figure 5, pH sensitivity after the deposition of a phospholipid monolayer is negligibly small (4.7 mV pH^{-1}).

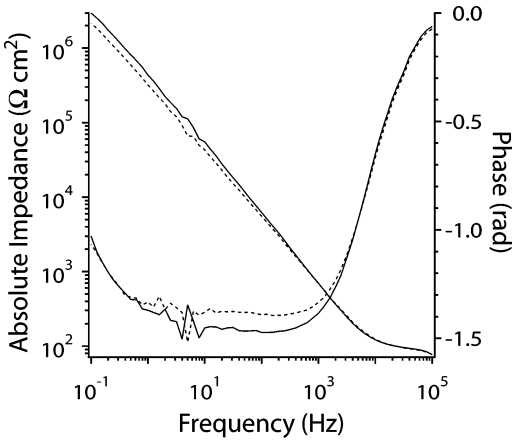

Figure 6. Enzymatic degradation of a phospholipid (DMPC) monolayer with PLA_2. The global shape of impedance spectra of the membrane-functionalized GaAs (solid lines) changes in 2 h after the injection of PLA_2, corresponding to the increase in D by almost 4 orders of magnitude.

The loss of pH sensitivity on a lipid monolayer can be attributed to the loss of short-range correlation in phosphocholine headgroups in the presence of cholesterol (40 mol %), in contrast to the CH_3-MBP monolayer that has almost no degree of conformational change.

Electrochemical Monitoring of Enzyme Functions. As the first step to monitor the biochemical reaction on the supported lipid monolayer on semiconductors electrochemically, we study the enzymatic activity of PLA_2 that cleaves the ester linkage of the *sn*-2 position of a glycerophospholipid and transfer it into a lysophospholipid and a fatty acid.[34] In Figure 6, we present the impedance of GaAs electrode with a DMPC monolayer (with 40 mol % of cholesterol) measured before the injection of PLA_2 (solid lines) and the impedance of the same sample measured after incubation with PLA_2 for 2 h at T = 25 °C (dashed lines). For these series of experiments, we replace the buffer from 10 mM Na_2HPO_4/NaH_2PO_4 to 10 mM Hepes to avoid undesired interference to the enzymatic activity.[35] The exchange of buffer salts does not cause any detectable change in the electrochemical parameters of the membrane in the absence of enzyme.

As can be seen in the figure, upon injection of PLA_2, the absolute impedance in the low-frequency region (f < 10 Hz), which is dominated by the Warburg resistance W_m shows a clear decrease after 2 h. This tendency can be interpreted as the decrease in the barrier capability of the membranes against the diffusion of ions, caused by the degradation of lipids by PLA_2.

In fact, the W_m value drops from the initial value, resulting in a significant increase in the diffusion coefficient of ions by 4 orders of magnitude, from $D_{(membrane)} = 5 \times 10^{-5}$ μm^2 s^{-1} to $D_{(membrane+PLA_2)} \approx 8 \times 10^{-1}$ μm^2 s^{-1}. The change in the diffusion barrier capability (i.e., leakiness) of the membrane agrees well with the previous reports using ellipsometry[29] and atomic force microscopy.[36,37] Furthermore, previously, Hønger et al. reported a high affinity of PLA_2 to phase boundaries between gel and fluid phases.[38] However, we do not carry out thorough investigations at the phase coexistence region, since the permeability of pure phospholipid membranes significantly increases around the phase transition temperature even in the absence of PLA_2.[39,40] Nevertheless, it should be noted that such a significant change in the membrane permeability still does not cause any electrochemical instability of the whole system, owing to the highly insulating CH_3-MBP monolayer.

Conclusions

Excellent electrochemical stability of GaAs achieved by covalent coupling of methyl-mercaptobiphenyl (CH_3-MBP) allows for the deposition of a lipid monolayer by fusion of small vesicles on the hydrophobic surface. Electrochemical impedance spectroscopy measurements over a wide frequency region (10^5-10^{-1} Hz) at the current minimum potential $U_{bias,j=0} = -400$ mV (vs Ag/AgCl) enables one to quantitatively identify electrochemical parameters of a supported lipid monolayer and those of the GaAs/CH_3-MBP interface with an aid of equivalent circuit models. The best fit results suggest that the presence of a lipid monolayer remarkably slows down the diffusion of ions, so that the electrochemical parameters of the membrane-functionalized GaAs remain stable for more than 3 days. The kinetics of membrane formation can be traced by monitoring the Warburg resistance Wm and capacitance C_m of the membrane, which can empirically be analyzed to gain the characteristic time constant of membrane formation.

Because of the quantitative identification of the resistance (R_p) and capacitance (C_p) of the GaAs/CH3-MBP interface even in the presence of a lipid monolayer, the change of the interface capacitance C_p that contains the contribution of the capacitance of semiconductor space charge region C_{SC} can be measured as functions of the surface charge density Q and bias potentials U_{bias}. The linear relationships obtained for $1/C_p^2$ vs Q and $1/C_p^2$ vs U_{bias} suggest that C_p can be used as a sensitive measure to detect the surface charges and that the charge sensitivity of the system can be calculated to be 1 charge per 18 nm^2. Moreover, preliminary experiments successfully demonstrate the potential application of membrane-functionalized semiconductor electrodes in the electrochemical monitoring of enzymatic reactions (degradation of phospholipids by PLA_2). The composite membranes established here open a large potential toward the design of new hybrid sensors by functionalization of various GaAs-based semiconductor devices with biological membranes.

Acknowledgment. This work has been supported by the Bundesministerium für Bildung and Forschung (BMBF) and the Fonds der Chemischen Industrie. D.G. thanks A. Stumpf (Walter Schottky Institute, Tech. Univ. Munich) for the technical assistance in the preparation of the electrodes.

References and Notes

(1) Cui, Y.; Wei, Q. Q.; Park, H. K.; Lieber, C. M. *Science* **2001**, *293*, 1289.
(2) Katz, E.; Willner, I. *Chem. Phys. Chem.* **2004**, *5*, 1085.
(3) Adachi, S. *J. Appl. Phys.* **1985**, *58*, R1.
(4) Joyce, B. A.; Vvedensky, D. D. *Mater. Sci. Eng. R* **2004**, *46*, 127.
(5) Pfeiffer, L. N.; West, K. W.; Willett, R. L.; Akiyama, H.; Rokhinson, L. P. *Bell Labs Tech. J.* **2005**, *10*, 151.
(6) Gerischer, H.; Mindt, W. *Electrochim. Acta* **1968**, *13*, 1329.
(7) Horowitz, G.; Allongue, P.; Cachet, H. *J. Electrochem. Soc.* **1984**, *131*, 2563.
(8) Menezes, S.; Miller, B. *J. Electrochem. Soc.* **1983**, *130*, 517.
(9) Adlkofer, K.; Tanaka, M.; Hillebrandt, H.; Wiegand, G.; Sackmann, E.; Bolom, T.; Deutschmann, R.; Abstreiter, G. *Appl. Phys. Lett.* **2000**, *76*, 3313.
(10) Adlkofer, K.; Tanaka, M. *Langmuir* **2001**, *17*, 4267.
(11) Adlkofer, K.; Eck, W.; Grunze, M.; Tanaka, M. *J. Phys. Chem. B* **2003**, *107*, 587.
(12) Adlkofer, K.; Shaporenko, A.; Zharnikov, M.; Grunze, M.; Ulman, A.; Tanaka, M. *J. Phys. Chem. B* **2003**, *107*, 11737.
(13) Luber, S. M.; Adlkofer, K.; Rant, U.; Ulman, A.; Golzhauser, A.; Grunze, M.; Schuh, D.; Tanaka, A.; Tornow, M.; Abstreiter, G. *Phys. E* **2004**, *21*, 1111.
(14) Gassull, D.; Luber, S. M.; Ulman, A.; Grunze, M.; Tornow, M.; Abstreiter, G.; Tanaka, M. *J. Phys. Chem. C* **2007**, *111*, 12414.
(15) Kang, J. F.; Ulman, A.; Liao, S.; Jordan, R.; Yang, G.; Liu, G. *Langmuir* **2001**, *17*, 95.
(16) Allongue, P.; Cachet, H. *Ber. Bunsen. Phys. Chem.* **1987**, *91*, 386.
(17) Hillebrandt, H.; Tanaka, M.; Sackmann, E. *J. Phys. Chem. B* **2002**, *106*, 477.
(18) Ho, C.; Raistrick, I. D.; Huggins, R. A. *J. Electrochem. Soc.* **1980**, *127*, 343.
(19) Finklea, H. O.; Snider, D. A.; Fedyk, J.; Sabatani, E.; Gafni, Y.; Rubinstein, I. *Langmuir* **1993**, *9*, 3660.
(20) MacDonald, J. R. *Impedance Spectroscopy*; John Wiley & Sons: New York, 1987.
(21) Hillebrandt, H.; Tanaka, M. *J. Phys. Chem. B* **2001**, *105*, 4270.
(22) Jensen, T. R.; Østergaard Jensen, M.; Reitzel, N.; Balashev, K.; Peters, G. H.; Kjaer, K.; Bjørnholm, T. *Phys. Rev. Lett.* **2003**, *90*, 086101.
(23) Doshi, D. A.; Watkins, E. B.; Israelachvili, J. N.; Majewski, J. *Proc. Natl. Acad. Sci. U.S.A.* **2005**, *102*, 9458.
(24) Dilger, J. P.; McLaughlin, S. G. A.; McIntosh, T. J.; Simon, S. A. *Science* **1979**, *206*, 1196.
(25) Montal, M.; Mueller, P. *Proc. Natl. Acad. Sci. U.S.A.* **1972**, *69*, 3561.
(26) Purrucker, O.; Hillebrandt, H.; Adlkofer, K.; Tanaka, M. *Electrochim. Acta* **2001**, *47*, 791.
(27) Requena, J.; Haydon, D. A. *Proc. R. Soc. London, Ser. A* **1975**, *347*, 161.
(28) Plant, A. L. *Langmuir* **1993**, *9*, 2764.
(29) Stelzle, M.; Weissmuller, G.; Sackmann, E. *J. Phys. Chem.* **1993**, *97*, 2974.
(30) Keller, C. A.; Glasmastar, K.; Zhdanov, V. P.; Kasemo, B. *Phys. Rev. Lett.* **2000**, *84*, 5443.
(31) *Phospholipids Handbook*; Cevc, G., Ed.; Marcel Dekker: New York, 1993.
(32) Sackmann, E.; Lipowski, R. *Structure and Dynamics of Membranes*; Elsevier: Amsterdam, The Netherlands, 1995.
(33) Sze, S. M. *Semiconductor Devices: Physics and Technology*; John Wiley & Sons: New York, 1985.
(34) Verger, R.; Mieras, M. C. E.; Dehaas, G. H. *J. Biol. Chem.* **1973**, *248*, 4023.
(35) Benes, M.; Billy, D.; Benda, A.; Speijer, H.; Hof, M.; Hermens, W. T. *Langmuir* **2004**, *20*, 10129.
(36) Balashev, K.; DiNardo, N. J.; Callisen, T. H.; Svendsen, A.; Bjornholm, T. *Biochim. Biophys. Acta* **2007**, *1768*, 90.
(37) Leidy, C.; Mouritsen, O. G.; Jorgensen, K.; Peters, N. H. *Biophys. J.* **2004**, *87*, 408.
(38) Hønger, T.; Jorgensen, K.; Biltonen, R. L.; Mouritsen, O. G. *Biochemistry* **1996**, *35*, 9003.
(39) Papahadjopoulos, D.; Watkins, J. C. *Biochim. Biophys. Acta* **1967**, 639.
(40) Caillé, A.; Pink, D.; Verteuil, F.; Zuckermann, M. J. *Can. J. Phys.* **1980**, *58*, 581.